Biophysical Chemistry 309 (2024) 107233

Contents lists available at ScienceDirect

Biophysical Chemistry

journal homepage: www.elsevier.com/locate/biophyschem

# New insights into the interaction of emodin with lipid membranes

Antonio R. da Cunha [a,b,*], Evandro L. Duarte [b], Gabriel S. Vignoli Muniz [b,c], Kaline Coutinho [b], M. Teresa Lamy [b]

[a] Universidade Federal do Maranhão, UFMA, Campus Balsas, 65800-000, Maranhão, Brazil
[b] Instituto de Física, Universidade de São Paulo, Cidade Universitária, São Paulo 05508-090, Brazil
[c] Instituto de Química, Universidade de Brasília, Campus Universitário Darcy Ribeiro, Brasília 70910-900, Brazil

ARTICLE INFO

*Keywords:*
Emodin
Lipid bilayer
Optical spectra
Lipid partition coefficient
Differential scanning calorimetry
ESR spectroscopy

ABSTRACT

Emodin is a natural anthraquinone derivative found in nature, widely known as an herbal medicine. Here, the partition, location, and interaction of emodin with lipid membranes of 1,2-dimyristoyl-sn-glycero-3-phosphocholine (DMPC) are experimentally investigated with different techniques. Our studies have considered the neutral form of emodin (EMH) and its anionic/deprotonated form ($EM^-$), and their interaction with a more and less packed lipid membrane, DMPC at the gel and fluid phases, respectively. Though DSC results indicate that the two species, EMH and $EM^-$, similarly disrupt the packing of DMPC bilayers, spin labels clearly show that EMH causes a stronger bilayer disruption, both in gel and fluid DMPC. Fluorescence spectroscopy shows that both EMH and $EM^-$ have a high affinity for DMPC: the binding of $EM^-$ to both gel and fluid DMPC bilayers was found to be quite similar, and similar to that of EMH to gel DMPC, $K_p = (1.4 \pm 0.3)x10^3$. However, EMH was found to bind twice more strongly to fluid DMPC bilayers, $K_p = (3.2 \pm 0.3)x10^3$. Spin labels and optical absorption spectroscopy indicate that emodin is located close to the lipid bilayer surface, and suggest that $EM^-$ is closer to the lipid/water interface than EMH, as expected. The present studies present a relevant contribution to the current understanding of the effect the two species of emodin, EMH and $EM^-$, present on different microregions of an organism, as local *pH* values can vary significantly, can cause in a neutral lipid membrane, either more or less packed, liked gel and fluid DMPC, respectively, and could be extended to lipid domains of biological membranes.

## 1. Introduction

Emodin (1,3,8-trihydroxy-6-methyl-9,10-anthraquinone, Fig. 1) is a natural pharmacophore extracted from medicinal herbs, such *Polygonum cuspidatum*, *Rheum palmatum*, *Polygonaceae*, and *Cassieae*, which are traditionally used in Chinese medicine [1–3]. It is a natural anthraquinone derivative, also known to have anti-cancer [4–8], antiviral [9–11], anti-bacterial [12–14], anti-inflammatory [15–18], diuretic and vasorelaxant effects [19–21]. Previous studies have revealed that emodin has anti-cancer efficacy in different cancer types, including cervical cancer [22], breast cancer [23], and tongue cancer [24]. Recent studies have indicated that emodin could induce apoptosis in many cancer cells, such as lung cancer cells [25], glioma stem cells [26] and colon cancer cells [27], and could also exhibit strong inhibitory effect on cancer cell migration [28] and invasion [29]. However, the real molecular mechanism and details regarding how emodin induces apoptosis and suppresses invasion and migration in cancer cells are still not clear.

The interaction of a pharmacophore with cell membranes is a topic of great interest in biology and pharmacology due to the fact that the absorption, distribution, metabolism, and excretion of a drug involve many types of interactions in its passage across the cell membrane [27,30–33]. A wide range of experimental techniques has been used to investigate the interaction of emodin with phospholipids and its effect on model membranes, like UV/Visible absorption [34] and fluorescence spectroscopy [35,36], differential scanning calorimetry (DSC) [35,37], nuclear magnetic resonance (NMR) [37,38], light scattering [35], infrared spectroscopy and X-ray powder diffraction [37].

Emodin is a small amphiphilic anthraquinone insoluble and displaying a yellow colour in water at acidic *pH*, but red and soluble in water at alkaline *pH*. Previous studies have shown that this noticeable change in colour of emodin in solution with different *pH* values is due to a deprotonation process [39–41]. Varying the *pH* of the solution from acidic to alkaline shifts the emodin optical low energy absorption/emission band by several tens of wavenumbers, due to the change of its

* Corresponding author at: Universidade Federal do Maranhão, UFMA, Campus Balsas, 65800-000, Maranhão, Brazil.
*E-mail address:* cunha.antonio@ufma.br (A.R. da Cunha).

https://doi.org/10.1016/j.bpc.2024.107233
Received 12 February 2024; Received in revised form 26 March 2024; Accepted 1 April 2024
Available online 2 April 2024

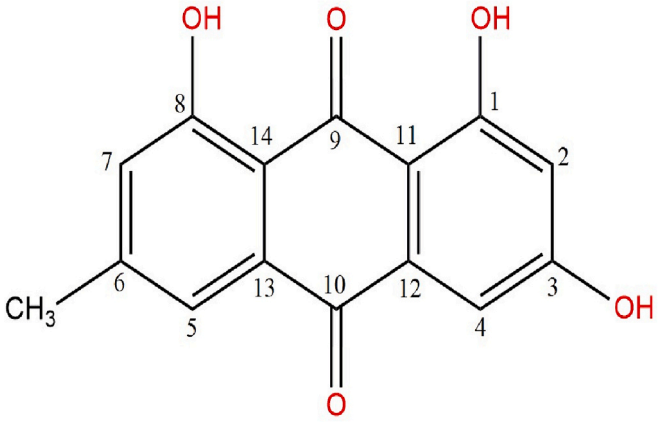


**Fig. 1.** Chemical structure and atomic numbering of the neutral form of emodin (EMH).

protonation state. Based on UV/Visible spectrophotometric titration technique, a $pK_a$ of 8.0 ± 0.1 was previously reported for emodin in water [41]. Thus, in aqueous solution, for acidic values of *pH* (< 7.0) emodin is mostly in its neutral form (EMH), but for alkaline values of *pH* (> 9.0) the anionic/deprotonated form of the emodin is prevalent ($EM^-$).

Therefore, in the present work we investigate the interaction of the two different species of emodin, EMH and $EM^-$, with membranes of 1,2-dimyristoyl-sn-glycero-3-phosphocholine (DMPC), used as a model system, considering that PC is ubiquitous in cell membranes. It is important to have in mind that different emodin protonation states are expected to be present in different microregions of an organism, as local *pH* values can vary significantly. And the polarity, or the electric charge of a molecule, usually plays an important role in its interaction with lipid membranes [42–44].

We chose 14-carbon atom chains DMPC because it makes possible to monitor the membrane in different conditions of packing by varying the temperature from 5 to 40 °C, as the gel-fluid transition of DMPC is around 23 °C. Hence, fluid and gel DMPC bilayers could somehow mimic different packing regions in a biological membrane.

By differential scanning calorimetry (DSC), the present work analyzes the effect of both species of emodin, EMH and $EM^-$, on the thermotropic behavior of DMPC membranes. The structural alterations these two emodin species cause on the membranes are monitored by electron spin resonance (ESR) of spin probes incorporated in the bilayer at different depths. Moreover, the location of the two emodin species, in both gel and fluid DMPC membranes, is discussed based on their optical spectra, and their membrane/water partition coefficient is evaluated by fluorescence spectroscopy.

## 2. Materials and methods

### 2.1. Reagents

1,2-dimiristoyl-sn-glycero-3-phosphocholine (DMPC) and the spin labels 1-palmitoyl2-(*n*-doxylstearoyl)-sn-glycero-3-phosphocholine (*n*-PCSL, *n* = 5 and 16) were obtained from Avanti Polar Lipids (Birmingham, AL, USA). Emodin ($C_{15}H_{10}O_5$, Fig. 1), sodium hydroxide (NaOH), hydrochloric acid (HCl), sodium bicarbonate ($NaHCO_3$), sodium carbonate ($Na_2CO_3$), sodium biphosphate monohydrate ($NaH_2PO_4.H_2O$), sodium phosphate dibasic heptahydrate ($Na_2HPO_4.7H_2O$), boric acid, acetic acid sodium salt trihydrate and the solvents were purchased from Sigma-Aldrich Co. (St. Louis, MO, USA). Emodin stock solution (10 mM) was prepared in ethanol/methanol (4:1) and stored at −20 °C. All reagents were used without further purification. Milli-Q water was used throughout.

### 2.2. Lipid dispersion preparation

Binary mixtures were prepared from a 10 mM DMPC (chloroform stock solution) and a 10 mM emodin (ethanol/methanol (4:1, *v:v*) stock solution) at the desired molar ratios. The organic solvents were dried under a stream of $N_2$ while slightly vortexed, forming a homogeneous thin film at the bottom of the vial. The films were left under reduced pressure for at least 2 h in order to remove all traces of organic solvents. For ESR measurements, 0.8 mol% of 5-PCSL or 0.3 mol% of 16-PCSL, relative to the lipid concentration, were added to the binary mixtures of lipid/emodin when preparing the films. No spin-spin interaction was identified for the spin label concentrations used.

Lipid dispersions were prepared by adding buffer solution to the films, vortexing and heating them at 30 °C, *i.e.*, above the DMPC gel-fluid phase transition temperature ($T_m$ = 23 °C) [45,46]. As DMPC in aqueous medium forms large multilamellar vesicles (LMVs) [47], which quickly precipitate, interfering in the optical absorption and emission spectroscopic results, for the samples containing DMPC, a process of extrusion was performed in order to reduce the polydispersity and increase the dispersion stability, resulting in a less turbid sample, with large unilamellar vesicles (LUVs). So, DMPC dispersions were extruded using a mini-extruder by Avanti Polar Lipids where the solution passed 31 times through polycarbonate filters with 100 nm pores (Whatman plc, Maidstone, Kent, UK), at 30 °C. All lipid dispersions were extruded, except those used on DSC experiments. Lipid dispersions containing predominantly one of the emodin species, EMH or $EM^-$, were obtained using buffers at different *pH* values, 6.0 or 10.0, respectively, as previously reported [34]: the lipid/emodin films were hydrated in sodium biphosphate/phosphate buffer (*pH* 6.0) or bicarbonate/carbonate buffer (*pH* 10.0).

### 2.3. UV/Vis spectrophotometry

Optical absorption measurements were performed with a Varian Cary 50 UV–Vis Spectrophotometer, at two different temperatures (15 °C and 30 °C), *i.e.*, at temperatures below and above the lipid phase transition of DMPC, controlled by a Cary Peltier thermostat. Samples were placed in quartz cuvettes 4.0 × 10 mm, the concentration of emodin was kept constant at 0.025 mM, and the lipid concentration varied from 0 to 2 mM. All spectral curves were subtracted from baselines obtained from samples without emodin.

### 2.4. Fluorescence measurements

Steady state fluorescence emission measurements were performed with a Varian Cary Eclipse Fluorescence spectrophotometer (Santa Clara, CA, USA), with a Peltier temperature controller. Samples at low *pH* were excited at 446 nm whereas the samples at high *pH* were excited at 519 nm. For all fluorescence measurements, the sample was placed in a quartz cuvette 4.0 × 10 mm, with the excitation optical pathway of 4.0 mm. The temperature was controlled with a Carry Peltier thermostat. We performed inner filter corrections to obtain accurate emission spectra, as previously reported [48–50] [51], and described below.

The inner filter correction was applied by using Eq. (1):

$$F_{corr}(\lambda) = F_{obs}(\lambda)10^{A_{exc}l}10^{A_{ems}l'} \quad (1)$$

where $F_{corr}(\lambda)$ and $F_{obs}(\lambda)$ are the corrected and observed fluorescence intensity at a given λ, $A_{exc}$ and $A_{ems}$ are the absorbance per unit of pathway at the excitation and emission wavelengths, respectively. $l$ and $l'$ are the optical pathways for excitation (0.2 cm), and for emission (0.5 cm), respectively, considering the cuvette center. The base line with pure DMPC was subtracted from the spectra before the due correction.

It is important to mention that the DMPC dispersion of LUVs, at the highest concentrations used here, causes a significant light scattering. A comparison between the uncorrected and corrected emission spectra of

emodin in DMPC vesicles is shown in Fig. SM1 in the Supplementary Material.

### 2.5. Determination of emodin partition into DMPC membranes

The apparent membrane partition coefficients, $K_p$, for the neutral and deprotonated species of emodin in DMPC membrane, were determined from the increase in the fluorescence intensity of these species in the presence of unilamellar vesicles, as compared with that in the aqueous phase. $K_p$ is defined as:

$$K_p = \frac{n_L/V_L}{n_{aq}/V_{aq}} \tag{2}$$

where $n_L$ and $n_{aq}$ are the number of moles of EMH or $EM^-$ in the lipid and aqueous phases, respectively. $V_{aq}$ is the volume of the aqueous phase which is in a good approximation equal to the total volume ($V_{total}$), taking into consideration both phases, aqueous and lipid. $V_L$ is the volume of the lipid phase.

The calculation of $K_p$ was done as described in the literature [52,53], using the following equation,

$$\Delta I = \frac{\Delta I_{max}[L]}{1/K_p\gamma + [L]} \tag{3}$$

where $\Delta I$ ($\Delta I = I - I_0$) stands for the difference between the fluorescence intensity of emodin measured in the presence ($I$) and in the absence of the phospholipid vesicles ($I_0$). $\Delta I_{max} = I_\infty - I_0$, where $I_\infty$ is the limiting value, upon increasing the phospholipid concentration [L], and $\gamma$ is the molar volume of the phospholipid membrane (for DMPC, in gel- and fluid-phases, the values of $\gamma$ are 0.62 and 0.70 $M^{-1}$, respectively [45]).

The concentration of emodin was kept constant at 0.025 mM, and phospholipid concentration was varied from 0 to 2 mM. The samples containing predominantly EMH at *pH* 6.0 and $EM^-$ at *pH* 10 were prepared in universal buffer (borate, acetate, phosphate), controlling the *pH* by the addition of NaOH and HCl at concentrations according to the desired *pH* value. The measurement of the fluorescence spectra of emodin were performed with DMPC vesicles in both gel phase, at 15 °C, and fluid phase, at 30 °C.

### 2.6. Differential scanning calorimetry (DSC)

DSC measurements were performed with a Microcalorimeter (Microcal VP-DSC, Northampton, MA, USA), controlled by the VP-viewer program and equipped with 0.5 mL twin total-fill cells. Samples were heated from 3 to 65 °C at a scan rate of 20 °C/h. Scans were performed at least in duplicate. Baseline subtractions and peak integrals were done using the Microcal Origin software with the additional pack for DSC data analysis provided by Microcal. DMPC concentration was fixed at 5 mM whereas emodin concentration was varied from 0 up to 20 mol% of emodin relative to the lipid concentration.

### 2.7. ESR spectroscopy

ESR measurements were performed with a Bruker EMX spectrometer, at X band (9.33 GHz). The sample temperature was controlled within 0.1 °C by a Bruker BVT2000 variable-temperature device and varied from 5 to 50 °C. To ensure thermal equilibrium, before each scan, the sample was left at the desired temperature for at least 10 min. The ESR data were acquired immediately after sample preparation. Field-modulation amplitude of 1 or 2 G and microwave power of 10 mW were used. The ESR spectra were analyzed using the software WINEPR. DMPC concentration was fixed at 10 mM whereas emodin concentration was varied from 0 up to 20 mol% of emodin relative to the lipid concentration.

Empirical parameters obtained directly from the spectra, give us information about dynamics, polarity and packing of the membrane. Accordingly, the maximum hyperfine splitting value, $A_{max}$, measured on the 5-PCSL spectrum (Fig. 6), decreases with the label increasing mobility. When the same spin label probes an ordered but more fluid environment, the minimum hyperfine splitting value, $A_{min}$, can be measured directly on the spectrum (Fig. 6). With both empirical parameters, the effective order parameter, $S_{eff}$, can be calculated as follow [54]:

$$S_{eff} = \frac{A_\parallel - A_\perp}{A_{zz} - (1/2)(A_{xx} + A_{yy})} \frac{a_0'}{a_0} \tag{4}$$

where $A_\parallel = A_{max}$, $A_\perp = A_{min} + 1.4\left[1 - \frac{A_\parallel - A_{min}}{A_{zz} - (1/2)(A_{xx}+A_{yy})}\right]$, and $A_{xx}$, $A_{yy}$ and $A_{zz}$ are the principal values of the hyperfine tensor for doxylpropane [55].

The experimental and theoretical isotropic hyperfine splitting, $a_0$ and $a_0'$ respectively, can be calculated from the expressions:

$$a_0 = (1/3)(A_\parallel + A_\perp)\ a_0' = (1/3)(A_{xx} + A_{yy} + A_{zz}). \tag{5}$$

For the spin label near the center of the bilayer, as 16-PCSL, the ratio between the low and central field line amplitudes ($h_{+1}/h_0$) and the high and central field line amplitudes ($h_{-1}/h_0$) are the best parameter to be directly taken from the spectra (see Fig. 6). Both ratios tend to unit when the viscosity at the microenvironment probed by the spin label decreases. For more details see [56].

## 3. Results and discussions

### 3.1. Effect of emodin on the gel-fluid thermal transition of DMPC membrane

The effect of emodin on the thermotropic behavior of DMPC membranes was investigated by using the technique of differential scanning calorimetry (DSC). Membrane gel-fluid thermal transition is a collective process which depends on lipid-lipid interaction and may be profoundly affected by an exogenous molecule if it alters the lipid bilayer packing. Therefore, DSC technique might provide information about possible structural modifications induced by emodin on membranes.

Several studies have investigated the effect of *pH* on pure DMPC membrane, at different temperatures. As expected, at *pH* values from 6 to 10, where PC displays no titratable group, there is almost no influence of *pH* on the structure and dynamics of the membrane: DMPC displays a rather sharp/cooperative gel-fluid transition around 23 °C, and a pretransition around 12 °C [57]. Fig. SM2, in the Supplementary Material, shows the DSC profiles of pure DMPC dispersions at both $pH = 6.0$ and $pH = 10.0$.

Fig. 2 shows the DSC profiles of DMPC dispersions in the absence and presence of emodin, at different concentrations of the anthraquinone (5, 10, 15, and 20 mol% relative to the lipid concentration), at both $pH = 6.0$ and $pH = 10.0$. Interesting to find that in the presence of the two species, either the non-charged EMH or the anionic $EM^-$, DMPC DSC profiles are rather similar. Table 1 shows that the measured DSC parameters are also similar, within their uncertainties: the DMPC gel-fluid transition temperature, $T_m$, and the transition enthalpy, $\Delta H$, for the different percentages of emodin. Accordingly, the DSC profiles are similar to those obtained for emodin at $pH = 7.4$, in DMPC membrane, by Alves et al. [35], where the predominant species should be EMH, considering the emodin $pK_a$ of 8.0 found by us [41]. Like many other molecules that bind to lipid membranes (see, for instance, barbaloin [35]), the binding of emodin to DMPC membranes makes the bilayer pretransition peak to disappear, and gradually broadens the main gel-fluid transition, till it nearly disappears with 20 mol% of emodin (see also Table 1). Hence, this is a clear indication that both species of emodin penetrate the DMPC bilayer, strongly disrupting the membrane

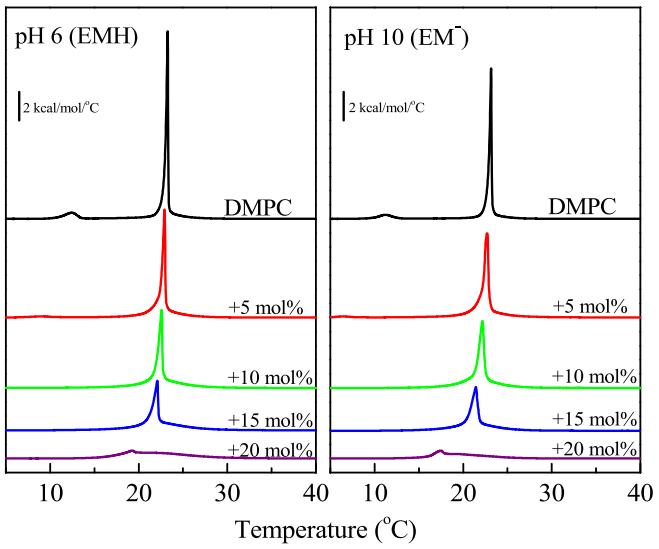


**Fig. 2.** Typical DSC heating thermograms of DMPC dispersions (5 mM) containing neutral emodin (EMH) at *pH* = 6.0, and anionic/deprotonated emodin ($EM^-$) at *pH* = 10.0, at different emodin/DMPC molar concentrations, as indicated.

**Table 1**
The DMPC gel-fluid transition temperature, $T_m$, and the transition enthalpy, $\Delta H$, obtained from DSC profiles in the presence of increasing amounts of emodin in the lipid dispersion. All data shown are means of the results of at least two experiments and the uncertainties are the standard deviations.

| emodin/DMPC (mol %) | *pH* 6 (EMH) | | *pH* 10 ($EM^-$) | |
|---|---|---|---|---|
| | $T_m$ (°C) | $\Delta H$ (kcal/mol) | $T_m$ (°C) | $\Delta H$ (kcal/mol) |
| 0 | 23.3 (±0.1) | 6.6 (±0.1) | 23.2 (±0.1) | 6 (±1) |
| 5 | 22.9 (±0.1) | 6.2 (±0.3) | 22.4 (±0.5) | 6 (±1) |
| 10 | 22.6 (±0.1) | 6.0 (±0.7) | 21 (±1) | 6 (±1) |
| 15 | 22.2 (±0.1) | 6.1 (±0.4) | 20 (±2) | 5 (±2) |
| 20 | 21 (±2) | 3 (±2) | 19 (±2) | 4.2 (±0.7) |

structure. Moreover, it is important to point out that the broadening of the DMPC gel-fluid transition indicates a homogeneous perturbation of the lipids due to emodin binding, decreasing the cooperativity of the transition. That is, there is no indication of the coexistence of emodin-bound and emodin-free regions (bulk lipid) in the bilayer, as observed with some molecules (see, for instance [48]).

### 3.2. Location of emodin in DMPC membranes by optical absorption spectroscopy

In a previous study, we discussed the location of $EM^-$ in fluid DMPC bilayers [34], considering the sensitivity of its optical absorption spectrum to the polarity of the microenvironment. Here, we found important to extend that work, discussing the optical absorption spectrum of the molecule in the presence of both gel (15 °C) and fluid (30 °C) phases of the membrane, to mimic different packing regions in a biological membrane, as mentioned above. Fig. 3 shows the UV/Visible spectra of emodin in aqueous buffer solution and in the presence of DMPC membrane (1 mM), at two different temperatures, $T = 15$ °C and $T = 30$ °C, *i.e.*, below and above the lipid gel-fluid phase transition ($T_m = 23$ °C), and at two different *pH* values, 6.0 and 10.0, where there is a high predominance of EMH and $EM^-$, respectively, considering the emodin $pK_a$ value of 8.0 [41].

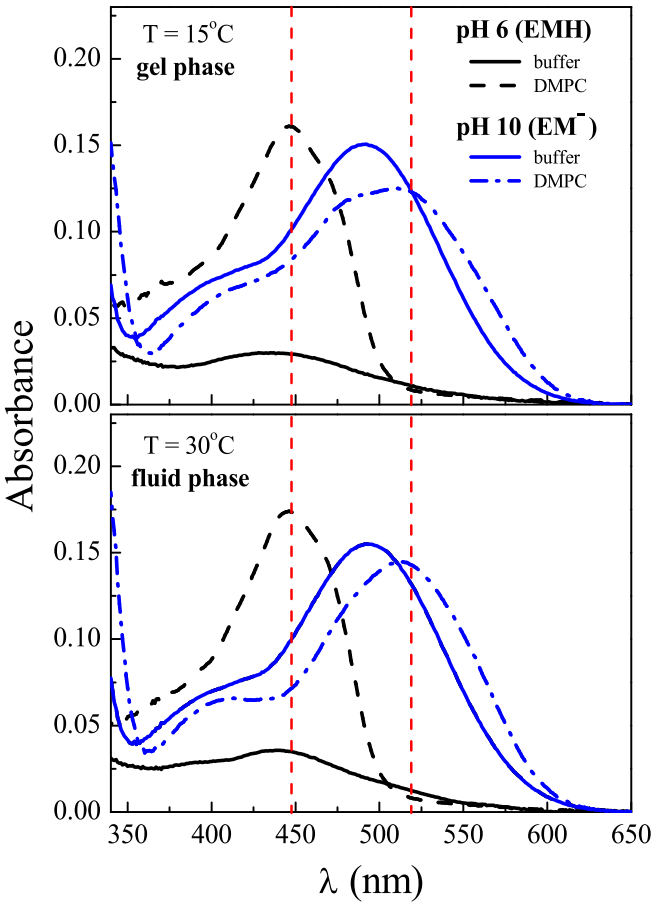


**Fig. 3.** Optical absorption spectra of 0.025 mM of emodin, neutral at *pH* 6.0 (EMH, black lines) and anionic at *pH* 10.0 ($EM^-$, blue lines), in buffer solution (solid lines) and in DMPC (1 mM) dispersion (dash lines and dash dot lines), at T = 15 °C (gel phase) and T = 30 °C (fluid phase). Emodin/DMPC = 2 mol%. Dashed vertical red lines are just guides for the eyes, drawn at wavelength values 446 and 519 nm. (For interpretation of the references to colour in this figure legend, the reader is referred to the web version of this article.)

As it is well known [34,39–41], EMH (*pH* 6) aggregates in aqueous solution, and displays a broad band around 450 nm (Fig. 3). However, Fig. 3 shows that it binds to both gel and fluid DMPC membranes, displaying a much well-defined optical absorption band around 446 nm (see Table 2). As discussed before [34], the optical absorption spectrum of EMH in the presence of DMPC membrane is similar to that of EMH in different solvents where it is not aggregated, but monomeric, as the spectrum is not sensitive to the medium polarity [41]. Accordingly, apart from the knowledge that monomeric EMH is imbedded in both gel and fluid DMPC membranes, no information about EMH position in the DMPC membrane can be obtained from its optical absorption spectrum.

**Table 2**
The wavelength at the maximum absorption intensity ($\lambda_{max}$ in nm) and molar absorptivity ($\varepsilon$ in $m^2$/mol) of the lowest energy band of EMH and $EM^-$ in buffer and in DMPC suspensions, at two different temperatures: $T = 15$ °C (gel phase) and $T = 30$ °C (fluid phase).

| Temperature | Medium | *pH* 6 (EMH) | | *pH* 10 ($EM^-$) | |
|---|---|---|---|---|---|
| | | $\lambda_{max}$ (nm) | $\varepsilon$ ($m^2$/mol) | $\lambda_{max}$ (nm) | $\varepsilon$ ($m^2$/mol) |
| 15 °C | buffer | ~* | 0.15 | 492 | 0.76 |
| | DMPC | 446 | 0.83 | 510 | 0.63 |
| 30 °C | buffer | ~ | 0.17 | 492 | 0.77 |
| | DMPC | 446 | 0.85 | 514 | 0.73 |

Opposite to that, the position of the maximum of the $EM^-$ absorption band was shown to be dependent on the medium polarity [41], its peak position shifting to higher wavelengths, lower energies, as $EM^-$ goes from water to less polar solvents. As discussed before, in fluid DMPC membranes, the $EM^-$ band position centered around 514 nm is lower than those obtained with emodin in ethanol, 2-propanol or acetonitrile [34], so the molecule chromophore moiety is supposed to be localized close to the bilayer interface, and not deep in the hydrocarbon chains. Fig. 3 shows that the optical absorption spectrum of $EM^-$ in both gel and fluid DMPC membranes is similar, but not identical: in DMPC gel phase, $EM^-$ lower energy band is slightly broader and shifted to higher energies as compared with the molecule in fluid bilayer (see also Table 2). That could be due to different hydration and/or packing of the two lipid phases, and/or to slightly different locations of the charged molecule in the membranes.

### 3.3. Structural changes caused by emodin in DMPC membrane monitored by ESR

Fig. 4 shows the ESR spectra of 5-PCSL and 16-PCSL inserted into gel (15 °C) and fluid (30 °C) DMPC membranes, in the absence (black lines) and presence (red lines) of 20 mol% of emodin (EMH or $EM^-$). The ESR spectra were also obtained at the emodin concentrations of 5, 10, 15 mol %, shown in the Supplementary Material (see Fig. SM3).

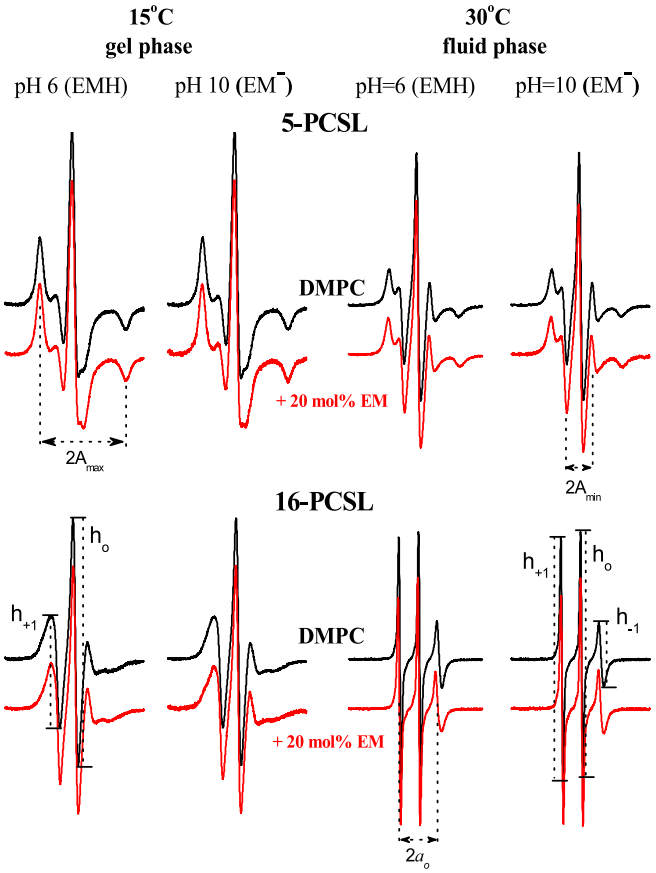


**Fig. 4.** ESR spectra of 5-PCSL (top lines) and 16-PCSL (bottom lines) embedded into pure 10 mM DMPC membranes (black lines), and DMPC in the presence of 20 mol% emodin (red lines), at *pH* 6.0 and 10.0, as indicated. The spectra were obtained with the membrane in the gel (15 °C) and fluid phases (30 °C). The maximum and minimum hyperfine splitting ($A_{max}$ and $A_{min}$, respectively), the isotropic hyperfine splitting ($a_o$) and the amplitudes of the features at low ($h_{+1}$,), central ($h_o$) and high ($h_{-1}$) field are indicated. The total spectra width is 100 G. (For interpretation of the references to colour in this figure legend, the reader is referred to the web version of this article.)

It is well established that spin-labels inserted into a lipid environment with high order, as the environment monitored by 5-PCSL in DMPC membranes, close to the bilayer surface, give rise to highly anisotropic ESR spectra. On the other hand, spin-labels located at the bilayer core, such as 16-PCSL, yield more isotropic spectra [55,56]. All these characteristics can be clearly observed by comparing the spectra of 5-PCSL and 16-PCSL in Fig. 4, in the absence or presence of emodin. Moreover, as expected, the spectra of both spin labels indicate a much more rigid environment in DMPC gel phase (15 °C) than in the fluid phase (30 °C).

As the possible changes induced by emodin on the bilayer structure cannot be easily evaluated by the simple observation of the ESR spectra, they were quantified by parameters directly measured on the spectra. Accordingly, Fig. 5 shows the appropriated empirical parameters [56] obtained from the ESR spectra with the spin-labels 5-PCSL and 16-PCSL inserted into the DMPC bilayer, in the absence and presence of emodin (EMH or $EM^-$), at different concentrations (5, 10, 15, and 20 mol%).

Let us first focus on the interaction of emodin with gel DMPC membranes. Fig. 5a shows the maximum hyperfine splitting ($A_{max}$) (see Fig. 4 and Material and methods). This parameter is very sensitive to changes of mobility and order of the bilayer in DMPC gel membranes [56]: $A_{max}$ increases when the spin-probe is in a more packed lipid environment. As for the bilayer core, the ESR spectra of 16-PCSL in gel bilayers can be analyzed monitoring the relative amplitude of the lines ($h_{+1}/h_o$, see Fig. 4), which gets close to the unit as the membrane gets less packed and/or ordered [56].

Accordingly, in gel DMPC membranes, EMH (*pH* 6) causes a significant increase in the $A_{max}$ parameter (Fig. 5a), indicating that the neutral molecule is penetrating into gel membrane, and stiffening the bilayer region close to the 5th carbon atom of the hydrocarbon chain. On the other hand, nearly no effect is observed in the presence of $EM^-$ (*pH* 10). Moreover, we observe in Fig. 5c that the value of $h_{+1}/h_o$ increases consistently upon the addition of EMH, compared to pure lipid. This result indicates that EMH is making the membrane more fluid, and/or less organized, in the hydrophobic core of the bilayer. $EM^-$ causes a similar effect, but much less strong. Similar effect has been observed

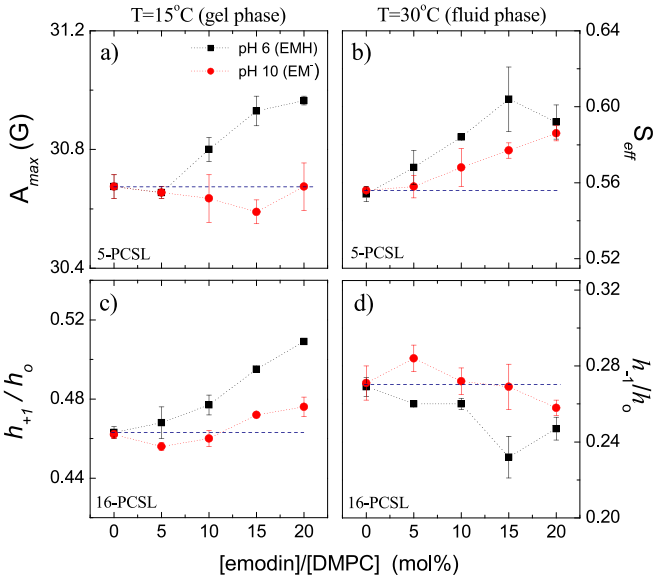


**Fig. 5.** Effect of emodin on the membrane structure of 10 mM DMPC, at *pH* 6.0 (black squares) and *pH* 10.0 (red circles), probed by 5-PCSL ($A_{max}$ and $S_{eff}$, for the gel and fluid phases, respectively) and 16-PCSL ($h_{+1}/h_o$ and $h_{-1}/h_o$, for the gel and fluid phases, respectively). (a) and (c) gel phase at 15 °C, and (b) and (d) fluid phase at 30 °C. The dashed lines are only guide for the eyes and represent the values obtained without emodin. (For interpretation of the references to colour in this figure legend, the reader is referred to the web version of this article.)

with other molecules bound close to the surface of packed gel membranes [58,59], indicating that the molecule would be inserted close to the bilayer surface, stiffening that region, and somehow spacing up the bilayer core.

For fluid DMPC membranes, with 5-PCSL, the best parameter to be used is the effective order ($S_{eff}$) parameter (see Fig. 4 and Material and methods), which can be understood as the orientation degree of the spin-probe relative to the bilayer normal. This parameter increases, and tends to 1, when the spin-probe gets more oriented parallel to the membrane normal, indicating an increase on the environmental order [56]. As for the bilayer core, the ESR spectra of 16-PCSL in fluid bilayers can be analyzed by the relative amplitude of the two lines corresponding to $m_I = -1$ and 0, $h_{-1}/h_o$ (see Fig. 4): $h_{-1}/h_o$ tends to unity as the probe movement becomes less ordered and faster [56].

In fluid DMPC membranes (30 °C; Fig. 5b), both species, EMH and EM$^-$, significantly increase $S_{eff}$, indicating that they penetrate the bilayer, increasing the bilayer order, EMH causing a stronger effect. At the bilayer core, EMH increases the packing (decreases the $h_{-1}/h_o$ ratio; Fig. 5d), with almost no effect observed with EM$^-$ at 30 °C. However, for higher temperatures, 50 °C, the presence of EM$^-$ clearly decreases the $h_{-1}/h_o$ ratio (Fig. SM4 and SM5), indicating that EM$^-$ also increases the packing of fluid DMPC.

To complement those results, the changes in the bilayer polarity, due to the presence of the molecules EMH and EM$^-$, were evaluated. It has been shown that, for spin labels inside a lipid bilayer, the magnitude of the nitrogen isotropic hyperfine splitting, $a_o$, is mainly related to the nitroxide-water hydrogen bonding [60]. Therefore, the extension of water presence into the bilayer can be estimated in fluid DMPC by the magnitude of $a_o$, either by directly measuring on an ESR spectrum like that of 16-PCSL in fluid DMPC, or by calculating from a spectrum like that of 5-PCSL in fluid DMPC (See Fig. 4). For 5-PCSL, as mentioned above, $a_o = (1/3)(A_{\parallel} + 2A_{\perp})$. It is not possible to directly measure $a_o$ in the ESR spectra of spin probes in gel membranes.

Fig. 6 shows that both species, EMH and EM$^-$, decreases the polarity of fluid DMPC at the bilayer core, measured with 16-PCSL, but have nearly no effect on the hydration closer to the bilayer surface, tested

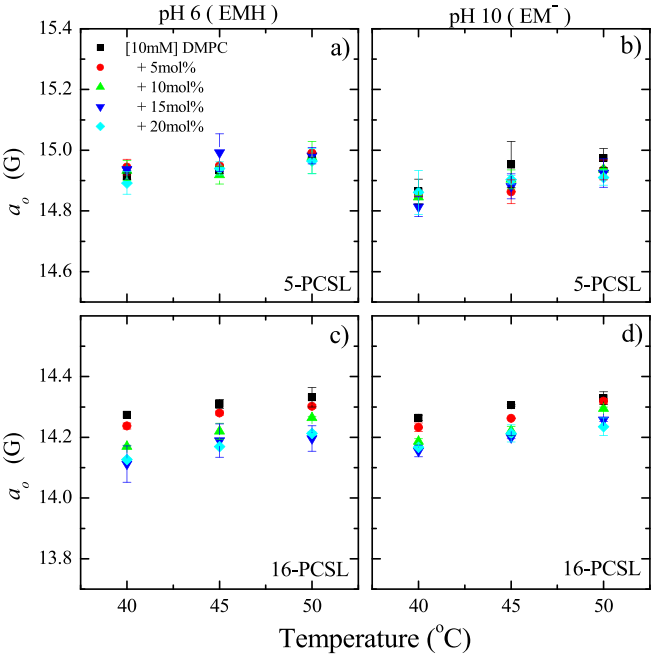


**Fig. 6.** Temperature dependence of the isotropic hyperfine splitting ($a_o$) measured on the ESR spectra of 5-PCSL ((a) and (b)) and 16-PCSL ((c) and (d)) incorporated in 10 mM DMPC at different emodin concentrations, as indicated, at *pH* 6.0 ((a) and (c)) and *pH* 10.0 ((b) and (d)).

with 5-PCSL. Here, again, the effect of EMH is more pronounced than that of EM$^-$. Hence, apart from getting more packed in the presence of emodin, the fluid DMPC bilayer core gets less hydrated (Fig. 6).

Hence, though the DMPC-DSC traces are not very different in the presence of EMH and EM$^-$ (see Fig. 2), spin probes indicate that EMH causes stronger structural changes on the DMPC membrane than the anionic species EM$^-$, both in the more packed gel phase of the membrane and in fluid bilayers. Also interesting, is to point out that although EMH absorption cannot distinguish if the neutral molecule is close to the surface or at the bilayer core, spin labels strongly indicate that, in the DMPC highly packed gel phase, EMH is deeper in the membrane, as discussed above.

It is interesting to compare those results with molecular dynamics (MD) simulations performed with both EMH and EM$^-$ in DMPC fluid bilayers in water medium [34]. In accord with our experimental results, the primary outcome of those simulations was that both EMH and EM$^-$ were found to be inside DMPC fluid bilayer, close to the glycerol groups, with EMH being slightly deeper in the bilayer, closer to the bilayer core. Also, in accord with the experimental results shown here, the bilayer disturbances found in the presence of EMH where more relevant than those found with charged EM$^-$. From [34], it can be seen that MD simulations indicate that, for the first carbon atoms, both EMH and EM$^-$ increase the bilayer chain order parameter, mainly that of chain sn-1. Our experimental results with 5-PCSL, which monitors that region, agree with those theoretical results, as they show an increase of $S_{eff}$ with the addition of both EMH and EM$^-$ (Fig. 5b). However, for the bilayer core, 16-PCSL shows a slight increase in the packing of that region (decrease of $h_{-1}/h_0$, Fig. 5d), while MD simulations indicate a decrease of the chains order parameter. Therefore, it can be concluded, that emodin, mainly EMH, possibly makes that region more packed but less ordered, that is the molecule disrupts the alignment of the chains relative to the normal to the bilayer.

To check whether the stronger effect detected by ESR with EMH is due to a stronger binding of EMH to DMPC, as compared with EM$^-$, membrane partition coefficients of EMH and EM$^-$ were calculated through fluorescence spectroscopy, as discussed below.

### 3.4. Partition of emodin in DMPC membrane: Fluorescence data

To investigate the partition of emodin in DMPC bilayers, measurements of emodin fluorescence emission were performed with the samples at the two *pH* values, 6.0 and 10.0, and under two different temperatures, 15 °C and 30 °C, *i.e.*, with the bilayer in the gel and fluid phases, respectively. Emodin fluorescence can only be detected in organic solvents or lipid bilayers. Though further studies are necessary, emodin is supposed to be monomeric in those solvents, as no self-quenching is detected.

It is interesting to have in mind that emodin in water at $pH = 6.0$, *i.e.*, EMH, aggregates and precipitates very fast, resulting in the quenching of the fluorescence intensity, as discussed before [36] [41]. The change of the emodin emission intensity observed in the presence of DMPC vesicles, as compared to that in aqueous phase, was used to quantify emodin DMPC partition coefficient, $K_p$ (Eq. (3)), from a procedure where DMPC concentration was varied from 0 to 2 mM and the concentration of emodin was kept constant, at 0.025 mM.

It is important to have in mind that those are effective $K_p$ values, as they measure an effective partition between emodin out of the membrane (either aggregated or in solution) and in the membrane. Hence, it is a good parameter for the comparison between the partition of EMH and EM$^-$ in membranes, considering the same total emodin concentrations, but it is not a good parameter for calculating the actual amount of bound emodin in the bilayer.

Fig. 7 shows the emission spectra of neutral (*pH* 6) and deprotonated/anionic (*pH* 10) species of emodin in DMPC dispersions at different lipid concentrations, at two temperatures (15 °C and 30 °C). In this figure, we observe an increase in the emission intensity upon

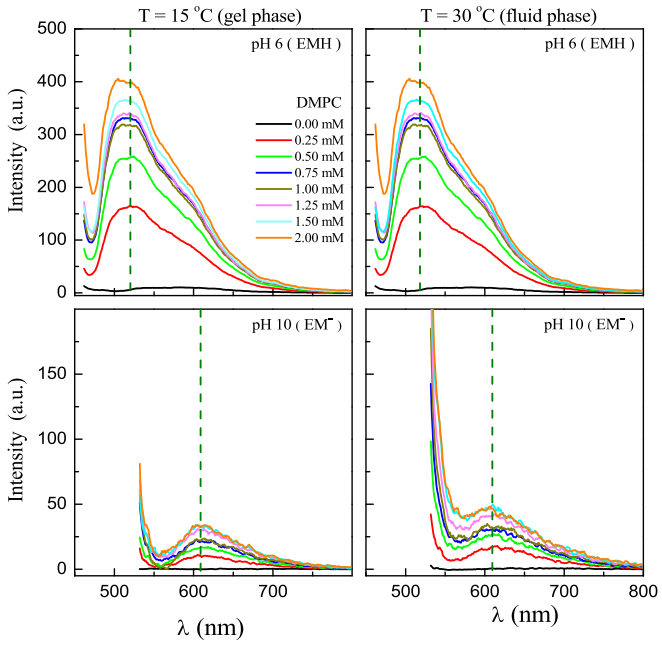


**Fig. 7.** Emission spectra of 0.025 mM neutral emodin (EMH) at $pH = 6.0$ and anionic/deprotonated emodin ($EM^-$) at $pH = 10.0$, in universal buffer and in DMPC dispersions at different lipid concentrations, for two different temperatures (15 °C and 30 °C). Spectra were corrected for the inner filter effect as discussed before [41–44]. The vertical dashed lines show the $\lambda_{max}$ of the emission band of emodin in phospholipid vesicles of DMPC, 520 nm (EMH) and 610 nm ($EM^-$). Excitation wavelengths were 446 nm for EMH and 519 nm for $EM^-$ (see Fig. 3).

addition of DMPC, clearly indicating the binding of the two forms of emodin to phospholipid bilayers, at both gel and fluid phases. Important to point out that the shape of the fluorescence spectrum does not change, just its amplitude (see Fig. SM6). That is a strong indication that the emodin bound species (either monomeric or aggregated) is the same for the whole experiment. The increase in the fluorescence emission of a fluorophore upon binding to lipid membranes in water medium could be due to both the reduction in non-radiative deactivation processes related with interactions between the fluorophore and the solvent molecules, and/or a decrease of the fluorophore's mobility. For EMH, the increase is mainly related to the reduction of the self-quench due to EMH aggregation in pure water medium.

Considering the fluorescence emission curves (see Fig. 7), we selected the emission wavelengths of 520 nm for EMH and 610 nm for $EM^-$ nm to perform the partition curves in terms of $\Delta I$, and used Eq. (3) to obtain the partition coefficients, $K_p$ (see Fig. 8). As defined in Section 2.5, $\Delta I$ ($\Delta I = I - I_0$) stands for the difference between the emission intensity of the emodin measured in the presence ($I$) and in the absence of DMPC vesicles ($I_0$). From the best fittings of Eq. (3) to the experimental data shown in Fig. 8, emodin partition coefficients into DMPC were obtained. For EMH, we obtained $K_p = (1.5 \pm 0.1)x10^3$ at $T = 15$ °C and $K_p = (3.2 \pm 0.3)x10^3$ at $T = 30$ °C. For the $EM^-$, we obtained $K_p = (1.4 \pm 0.3)x10^3$ at $T = 15$ °C and $K_p = (1.5 \pm 0.5)x10^3$ at $T = 30$ °C. Hence, the binding of $EM^-$ to gel and fluid DMPC bilayers was found to be quite similar, and like the binding of EMH to gel DMPC. But EMH binds twice more strongly to fluid DMPC bilayers. It is important to mention that $K_p$ values obtained here are much lower than that previously obtained by Alves et al. [35]. Fluorophores are sensitive to changes in the polarity of their surrounding environment, and this sensitivity is often exploited in fluorescence spectroscopy to probe the local environment or study molecular interactions. When a fluorophore goes from an aqueous environment to a lipid bilayer, a significant blue shift in its fluorescence band is expected as a result of the decrease in dipolar relaxation [61].

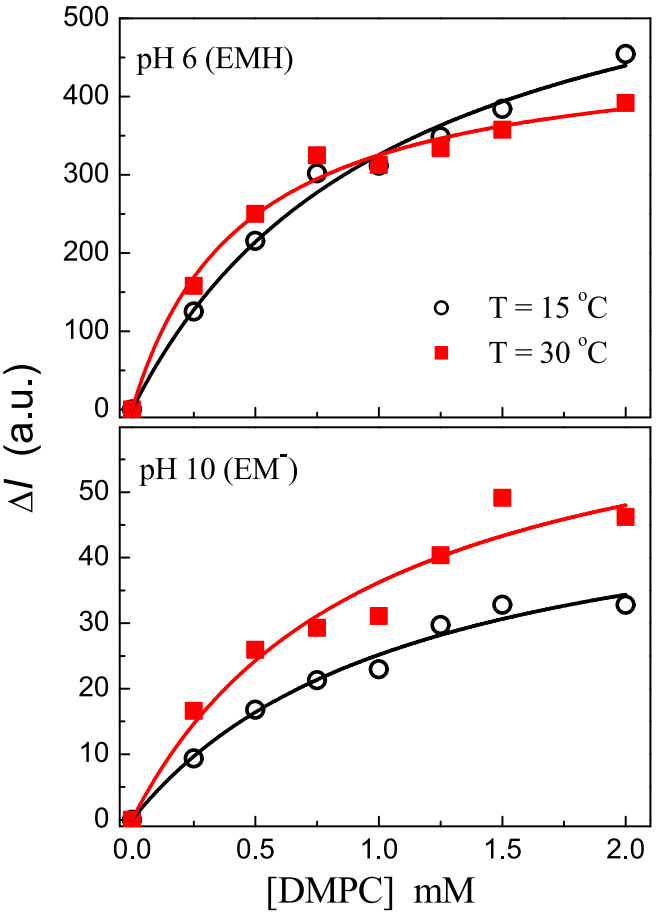


**Fig. 8.** Variation of $\Delta I$ for neutral Emodin (EMH), $pH = 6.0$, at 520 nm, and for the anionic/deprotonated Emodin ($EM^-$), $pH = 10.0$, at 610 nm, as a function of DMPC concentration, at two different temperatures (15 °C and 30 °C). $\Delta I$($\Delta I = I - I_0$) represents the difference between the emission intensity of the emodin measured in the presence ($I$) and in the absence ($I_0$) of phospholipid vesicles. The partition coefficient values, $K_p$, were obtained from the best fitting of Eq. (3) to experimental data.

However, as EMH does not fluoresce in aqueous solution, there is a lack of information regarding changes in its surrounding polarity through its emission.

ESR results which indicated stronger structural alterations caused by EMH to gel DMPC bilayers, as compared with $EM^-$, is not due to a stronger binding of EMH to the membrane, but most likely to a deeper penetration of the neutral molecule into the bilayer. As for fluid DMPC membranes, ESR results could be reflecting both effects: a deeper penetration of the neutral species EMH and its stronger DMPC binding.

## 4. Conclusions

The interaction of emodin with DMPC membranes, and its partition and location into lipid membranes, were explored here based on different experimental techniques: DSC, ESR spectroscopy, UV/Vis absorption and fluorescence spectroscopy. Our results indicate that both, neutral (EMH) and anionic/deprotonated form ($EM^-$) of emodin present a high affinity for DMPC membranes: the binding of $EM^-$ to both gel and fluid DMPC bilayers was found to be quite similar, and similar to that of EMH to gel DMPC, $K_p = (1.4 \pm 0.3)x10^3$. However, EMH was found to bind twice more strongly to fluid DMPC bilayers, $K_p = (3.2 \pm 0.3)x10^3$.

Though DSC results indicate that the two species, EMH and $EM^-$, similarly disrupt the packing of DMPC bilayers, spin labels clearly show that EMH causes a stronger bilayer disruption, both in gel and fluid DMPC. The analysis of the spin labels ESR spectra in the presence and

absence of emodin, strongly suggest that emodin in a lipid highly packed environment, like a gel membrane, is localized close to the water-bilayer interface, increasing the packing around the bilayer surface, but spacing up the lipids, hence making the bilayer core more fluid. In a lipid less packed environment, like fluid DMPC bilayers, emodin penetrates, increases the packing and decreases the presence of water molecules at the bilayer core.

In conclusion, our present experimental and past theoretical [34] studies bring a relevant contribution to the current understanding of the effect the two species of emodin, EMH and $EM^{-}$, present in different microregions of an organism, as local *pH* values can vary significantly, can cause in a neutral lipid membrane, either more or less packed, liked gel and fluid DMPC, respectively. Those results can possibly be extended to lipid domains of biological membranes.

## CRediT authorship contribution statement

**Antonio R. da Cunha:** Conceptualization, Investigation, Methodology, Data curation, Software, Writing – original draft. **Evandro L. Duarte:** Data curation, Investigation, Software. **Gabriel S. Vignoli Muniz:** Data curation, Investigation, Software. **Kaline Coutinho:** Data curation, Investigation, Resources, Software, Writing – review & editing. **M. Teresa Lamy:** Conceptualization, Methodology, Investigation, Resources, Writing – review & editing, Supervision.

## Declaration of competing interest

The authors declare that they have no known competing financial interests or personal relationships that could have appeared to influence the work reported in this paper.

## Data availability

Data will be made available on request.

## Acknowledgement

We acknowledge the financial support of the São Paulo Research Foundation (FAPESP 2017/25930-1; 2021/01593-1; 2021/09016-3) and the National Council for Scientific and Technological Development (CNPq – 465259/2014-6), the Coordination for the Improvement of Higher Education Personnel (CAPES), the National Institute of Science and Technology Complex Fluids (INCT-FCx), and the São Paulo Research Foundation (FAPESP – 2014/50983-3). A.R.C. thanks CNPq for a Graduate Scholarship, grant 156287/2010-2, 150171/2015-3. M. T.L. and K.C. also thank CNPq for research fellowships.

## Appendix A. Supplementary data

Supplementary data to this article can be found online at https://doi.org/10.1016/j.bpc.2024.107233.

## References

[1] R.H. Thomson, Naturally Occurring Quinones, 3nd ed., Chapman and Hall, London and New York, 1987.
[2] I. Izhaki, Emodin – a secondary metabolite with multiple ecological functions in higher plants, New Phytol. 155 (2002) 205–217, https://doi.org/10.1046/j.1469-8137.2002.00459.x.
[3] X. Dong, J. Fu, X. Yin, S. Cao, X. Li, L. Lin, J. Ni Huyiligeqi, Emodin: a review of its pharmacology, toxicity and pharmacokinetics, Phyther. Res. 30 (2016) 1207–1218, https://doi.org/10.1002/ptr.5631.
[4] Y.-C. Chen, S.-C. Shen, W.-R. Lee, F.-L. Hsu, H.-Y. Lin, C.-H. Ko, S.-W. Tseng, Emodin induces apoptosis in human promyeloleukemic HL-60 cells accompanied by activation of caspase 3 cascade but independent of reactive oxygen species production, Biochem. Pharmacol. 64 (2002) 1713–1724, https://doi.org/10.1016/S0006-2952(02)01386-2.
[5] G. Srinivas, R.J. Anto, P. Srinivas, S. Vidhyalakshmi, V.P. Senan, D. Karunagaran, Emodin induces apoptosis of human cervical cancer cells through poly(ADP-ribose) polymerase cleavage and activation of caspase-9, Eur. J. Pharmacol. 473 (2003) 117–125, https://doi.org/10.1016/S0014-2999(03)01976-9.
[6] W.-T. Wei, S.-Z. Lin, D.-L. Liu, Z.-H. Wang, The distinct mechanisms of the antitumor activity of emodin in different types of cancer (review), Oncol. Rep. 30 (2013) 2555–2562, https://doi.org/10.3892/or.2013.2741.
[7] F. Li, X. Song, X. Zhou, L. Chen, J. Zheng, Emodin attenuates high lipid-induced liver metastasis through the AKT and ERK pathways in vitro in breast cancer cells and in a mouse xenograft model, Heliyon 9 (2023) e17052, https://doi.org/10.1016/j.heliyon.2023.e17052.
[8] P.S. Lande, V.S. Adhao, J.P. Ambhore, K.P. Gaikwad, C.S. Chandak, L.P. Joge, Anticancer action of naturally occurring emodin for the controlling of cervical cancer, Explor. Target. Anti-Tumor Ther. (2023) 690–698, https://doi.org/10.37349/etat.2023.00161.
[9] D.L. Barnard, J.H. Huffman, J.L.B. Morris, S.G. Wood, B.G. Hughes, R.W. Sidwell, Evaluation of the antiviral activity of anthraquinones, anthrones and anthraquinone derivatives against human cytomegalovirus, Antivir. Res. 17 (1992) 63–77, https://doi.org/10.1016/0166-3542(92)90091-I.
[10] K. Kiyoshi, K. Taketoshi, M. Hideki, K. Jiro, N. Yoshinori, A comparative study on cytotoxicities and biochemical properties of anthraquinone mycotoxins emodin and skyrin from Penicillium islandicum sopp, Toxicol. Lett. 20 (1984) 155–160, https://doi.org/10.1016/0378-4274(84)90141-3.
[11] S. Schwarz, K. Wang, W. Yu, B. Sun, W. Schwarz, Emodin inhibits current through SARS-associated coronavirus 3a protein, Antivir. Res. 90 (2011) 64–69, https://doi.org/10.1016/j.antiviral.2011.02.008.
[12] H. Anke, I. Kolthoum, H. Laatsch, Metabolic products of microorganisms. 192. The anthraquinones of the Aspergillusglaucus group. II. Biological activity, Arch. Microbiol. 126 (1980) 231–236, https://doi.org/10.1007/BF00409925.
[13] H.-H. Wang, J.-G. Chung, Emodin-induced inhibition of growth and DNA damage in the *Helicobacter pylori*, Curr. Microbiol. 35 (1997) 262–266, https://doi.org/10.1007/s002849900250.
[14] D. Dey, R. Ray, B. Hazra, Antitubercular and antibacterial activity of Quinonoid natural products against multi-drug resistant clinical isolates, Phyther. Res. 28 (2014) 1014–1021, https://doi.org/10.1002/ptr.5090.
[15] A. Kumar, S. Dhawan, B.B. Aggarwal, Emodin (3-methyl-1,6,8-trihydroxyanthraquinone) inhibits TNF-induced NF-kB activation, IkB degradation, and expression of cell surface adhesion proteins in human vascular endothelial cells, Oncogene 17 (1998) 913–918, https://doi.org/10.1038/sj.onc.1201998.
[16] Y.-C. Kuo, H.-C. Meng, W.-J. Tsai, Regulation of cell proliferation, inflammatory cytokine production and calcium mobilization in primary human T lymphocytes by emodin from Polygonum hypoleucum Ohwi, Inflamm. Res. 50 (2001) 73–82, https://doi.org/10.1007/s000110050727.
[17] J.-K. Hwang, E.-M. Noh, S.-J. Moon, J.-M. Kim, K.-B. Kwon, B.-H. Park, Y.-O. You, B.-M. Hwang, H.-J. Kim, B.-S. Kim, S.-J. Lee, J.-S. Kim, Y.-R. Lee, Emodin suppresses inflammatory responses and joint destruction in collagen-induced arthritic mice, Rheumatology 52 (2013) 1583–1591, https://doi.org/10.1093/rheumatology/ket178.
[18] F. Yu, N. Yu, J. Peng, Y. Zhao, L. Zhang, X. Wang, X. Xu, J. Zhou, F. Wang, Emodin inhibits lipid accumulation and inflammation in adipose tissue of high-fat diet-fed mice by inducing M2 polarization of adipose tissue macrophages, FASEB J. 35 (2021), https://doi.org/10.1096/fj.202100157RR.
[19] M. Koyama, T.R. Kelly, K.A. Watanabe, Novel type of potential anticancer agents derived from chrysophanol and emodin. Some structure-activity relationship studies, J. Med. Chem. 31 (1988) 283–284, https://doi.org/10.1021/jm00397a002.
[20] X.M. Zhou, Q.H. Chen, Biochemical study of Chinese rhubarb. XXII. Inhibitory effect of anthraquinone derivatives on Na+-K+-ATPase of the rabbit renal medulla and their diuretic action, Yao Xue Xue Bao 23 (1988) 17–20.
[21] H. Huei-Chen, C. Shu-Hsun, P.-D.L. Chao, Vasorelaxants from Chinese herbs, emodin and scoparone, possess immunosuppressive properties, Eur. J. Pharmacol. 198 (1991) 211–213, https://doi.org/10.1016/0014-2999(91)90624-Y.
[22] W. Yaoxian, Y. Hui, Z. Yunyan, L. Yanqin, G. Xin, W. Xiaoke, Emodin induces apoptosis of human cervical cancer hela cells via intrinsic mitochondrial and extrinsic death receptor pathway, Cancer Cell Int. 13 (2013) 71, https://doi.org/10.1186/1475-2867-13-71.
[23] P.-H. Huang, C.-Y. Huang, M.-C. Chen, Y.-T. Lee, C.-H. Yue, H.-Y. Wang, H. Lin, Emodin induces apoptosis of human cervical cancer hela cells via intrinsic mitochondrial and extrinsic death receptor pathway. Evidence-based complement, Altern. Med. 2013 (2013) 71, https://doi.org/10.1155/2013/376123.
[24] Y.-Y. Chen, S.-Y. Chiang, J.-G. Lin, Y.-S. Ma, C.-L. Liao, S.-W. Weng, T.-Y. Lai, J.-G. Chung, Emodin, aloe-emodin and rhein inhibit migration and invasion in human tongue cancer SCC-4 cells through the inhibition of gene expression of matrix metalloproteinase-9, Int. J. Oncol. 36 (2010) 1113–1120, https://doi.org/10.3892/ijo_00000593.
[25] J. Su, Y. Yan, J. Qu, X. Xue, Z. Liu, H. Cai, Emodin induces apoptosis of lung cancer cells through ER stress and the TRIB3/NF-κB pathway, Oncol. Rep. 37 (2017) 1565–1572, doi: 110.3892/or.2017.5428.
[26] J. Kim, J.-S. Lee, J. Jung, I. Lim, J.-Y. Lee, M.-J. Park, Emodin suppresses maintenance of Stemness by augmenting Proteosomal degradation of epidermal growth factor receptor/epidermal growth factor receptor variant III in glioma stem cells, Stem Cells Dev. 24 (2015) 284–295, https://doi.org/10.1089/scd.2014.0210.
[27] K.H. Lee, M.S. Lee, E.Y. Cha, J.Y. Sul, J.S. Lee, J.S. Kim, J.B. Park, J.Y. Kim, Inhibitory effect of emodin on fatty acid synthase, colon cancer proliferation and apoptosis, Mol. Med. Rep. 15 (2017) 2163–2173, https://doi.org/10.3892/mmr.2017.6254.

[28] Q. Huang, H.-M. Shen, C.-N. Ong, Emodin inhibits tumor cell migration through suppression of the phosphatidylinositol 3-kinase-Cdc42/Rac1 pathway, C, Cell. Mol. Life Sci. 62 (2005) 1167–1175, https://doi.org/10.1007/s00018-005-5050-2.
[29] Q. Huang, H.-M. Shen, C.-N. Ong, Inhibitory effect of emodin on tumor invasion through suppression of activator protein-1 and nuclear factor-κB, Biochem. Pharmacol. 68 (2004) 361–371, https://doi.org/10.1016/j.bcp.2004.03.032.
[30] T.R. Oliveira, C.R. Benatti, M.T. Lamy, Structural characterization of the interaction of the polyene antibiotic amphotericin B with DODAB bicelles and vesicles, Biochim. Biophys. Acta Biomembr. 2011 (1808) 2629–2637, https://doi.org/10.1016/j.bbamem.2011.07.042.
[31] C. Bourgaux, P. Couvreur, Interactions of anticancer drugs with biomembranes: what can we learn from model membranes? J. Control. Release 190 (2014) 127–138, https://doi.org/10.1016/j.jconrel.2014.05.012.
[32] J. Knobloch, D.K. Suhendro, J.L. Zieleniecki, J.G. Shapter, I. Köper, Membrane–drug interactions studied using model membrane systems, Saudi, Aust. J. Biol. Sci. 22 (2015) 714–718, https://doi.org/10.1016/j.sjbs.2015.03.007.
[33] A.C. Alves, D. Ribeiro, C. Nunes, S. Reis, Biophysics in cancer: the relevance of drug-membrane interaction studies, Biochim. Biophys. Acta Biomembr. 2016 (1858) 2231–2244, https://doi.org/10.1016/j.bbamem.2016.06.025.
[34] A.R. da Cunha, E.L. Duarte, H. Stassen, M.T. Lamy, K. Coutinho, Experimental and theoretical studies of emodin interacting with a lipid bilayer of DMPC, Biophys. Rev. 9 (2017) 729–745, https://doi.org/10.1007/s12551-017-0323-1.
[35] D.S. Alves, L. Pérez-Fons, A. Estepa, V. Micol, Membrane-related effects underlying the biological activity of the anthraquinones emodin and barbaloin, Biochem. Pharmacol. 68 (2004), https://doi.org/10.1016/j.bcp.2004.04.012.
[36] P. Sevilla, F. García-Blanco, J.V. García-Ramos, S. Sánchez-Cortés, Aggregation of antitumoral drug emodin on ag nanoparticles: SEF, SERS and fluorescence lifetime experiments, Phys. Chem. Chem. Phys. 11 (2009) 8342–8348, https://doi.org/10.1039/B903935J.
[37] D. Singh, M.S.M. Rawat, A. Semalty, M. Semalty, Emodin-phospholipid complex, J. Therm. Anal. Calorim. 108 (2012) 289–298, https://doi.org/10.1007/s10973-011-1759-3.
[38] O.Y. Selyutina, P.A. Kononova, N.E. Polyakov, Experimental and theoretical study of Emodin interaction with phospholipid bilayer and linoleic acid, Appl. Magn. Reson. 51 (2020) 951–960, https://doi.org/10.1007/s00723-020-01233-x.
[39] T. Pal, N.R. Jana, Emodin (1,3,8-trihydroxy-6-methylanthraquinone): a spectrophotometric reagent for the determination of beryllium(II), magnesium(II) and calcium(II), Analyst 118 (1993) 1337, https://doi.org/10.1039/an9931801337.
[40] S.C. Nguyen, B.K. Vilster Hansen, S.V. Hoffmann, J. Spanget-Larsen, Electronic states of emodin and its conjugate base. Synchrotron linear dichroism spectroscopy and quantum chemical calculations, Chem. Phys. 352 (2008) 167–174, https://doi.org/10.1016/j.chemphys.2008.06.007.
[41] A.R. da Cunha, E.L. Duarte, M.T. Lamy, K. Coutinho, Protonation/deprotonation process of Emodin in aqueous solution and pKa determination: UV/visible spectrophotometric titration and quantum/molecular mechanics calculations, Chem. Phys. 440 (2014), https://doi.org/10.1016/j.chemphys.2014.06.009.
[42] C. Peetla, A. Stine, V. Labhasetwar, Biophysical interactions with model lipid membranes: applications in drug discovery and drug delivery, Mol. Pharm. 6 (2009) 1264–1276, https://doi.org/10.1021/mp9000662.
[43] H. Omote, M.K. Al-Shawi, Interaction of transported drugs with the lipid bilayer and P-glycoprotein through a solvation exchange mechanism, Biophys. J. 90 (2006) 4046–4059, https://doi.org/10.1529/biophysj.105.077743.
[44] M. Meier, X.L. Blatter, A. Seelig, J. Seelig, Interaction of verapamil with lipid membranes and P-glycoprotein: connecting thermodynamics and membrane structure with functional activity, Biophys. J. 91 (2006) 2943–2955, https://doi.org/10.1529/biophysj.106.089581.
[45] D. Marsh, CRC Handbook of Lipid Bilayers, CRC Press, Boca Raton, 1990.
[46] T. Heimburg, Thermal Biophysics of Membranes, Wiley-VCH, Weinheim, 2007.
[47] T.A. Enoki, V.B. Henriques, M.T. Lamy, Light scattering on the structural characterization of DMPG vesicles along the bilayer anomalous phase transition, Chem. Phys. Lipids 165 (2012) 826–837, https://doi.org/10.1016/j.chemphyslip.2012.11.002.
[48] T.A. Enoki, I. Moreira-Silva, E.N. Lorenzon, E.M. Cilli, K.R. Perez, K.A. Riske, M. T. Lamy, Antimicrobial peptide K0-W6-Hya1 induces stable structurally modified lipid domains in anionic membranes, Langmuir 34 (2018) 2014–2025, https://doi.org/10.1021/acs.langmuir.7b03408.
[49] S.A. Tucker, V.L. Amszi, W.E. Acree, Primary and secondary inner filtering. Effect of K2Cr2O7 on fluorescence emission intensities of quinine sulfate, J. Chem. Educ. 69 (1992) A8, https://doi.org/10.1021/ed069pA8.
[50] A. Mendonça, A.C. Rocha, A.C. Duarte, E.B.H. Santos, The inner filter effects and their correction in fluorescence spectra of salt marsh humic matter, Anal. Chim. Acta 788 (2013), https://doi.org/10.1016/j.aca.2013.05.051.
[51] J.R. Lakowicz, Principles of Fluorescence Spectroscopy, Springer, US, 2011. https://books.google.com.br/books?id=3QKTAQAACAAJ.
[52] C.R. Mateo, M. Prieto, V. Micol, S. Shapiro, J. Villalaín, A fluorescence study of the interaction and location of (+)-totarol, a diterpenoid bioactive molecule, in model membranes, Biochim. Biophys. Acta Biomembr. 1509 (2000) 167–175, https://doi.org/10.1016/S0005-2736(00)00291-1.
[53] N. Caturla, E. Vera-Samper, J. Villalaín, C.R. Mateo, V. Micol, The relationship between the antioxidant and the antibacterial properties of galloylated catechins and the structure of phospholipid model membranes, Free Radic. Biol. Med. 34 (2003) 648–662, https://doi.org/10.1016/S0891-5849(02)01366-7.
[54] J.M. Boggs, G. Rangaraj, Phase transitions and fatty acid spin label behavior in interdigitated lipid phases induced by glycerol and polymyxin, Biochim. Biophys. Acta Biomembr. 816 (1985) 221–233, https://doi.org/10.1016/0005-2736(85)90489-4.
[55] W.L. McConnell, M. Harden, Hubbell, Molecular motion in spin-labeled phospholipids and membranes, J. Am. Chem. Soc. 93 (1971) 314–326, https://doi.org/10.1021/ja00731a005.
[56] J.H.K. Rozenfeld, E.L. Duarte, T.R. Oliveira, M.T. Lamy, Structural insights on biologically relevant cationic membranes by ESR spectroscopy, Biophys. Rev. 9 (2017) 633–647, https://doi.org/10.1007/s12551-017-0304-4.
[57] H. Pruchnik, D. Bonarska-Kujawa, H. Kleszczyńska, Effect of chlorogenic acid on the phase transition in phospholipid and phospholipid/cholesterol membranes, J. Therm. Anal. Calorim. 118 (2014) 943–950, https://doi.org/10.1007/s10973-014-3841-0.
[58] E.L. Duarte, T.R. Oliveira, D.S. Alves, V. Micol, M.T. Lamy, On the interaction of the Anthraquinone Barbaloin with negatively charged DMPG bilayers, Langmuir 24 (2008), https://doi.org/10.1021/la703896w.
[59] L.G.M. Basso, R.Z. Rodrigues, R.M.Z.G. Naal, A.J. Costa-Filho, Effects of the antimalarial drug primaquine on the dynamic structure of lipid model membranes, Biochim. Biophys. Acta Biomembr. 2011 (1808) 55–64, https://doi.org/10.1016/j.bbamem.2010.08.009.
[60] O.H. Griffith, P.J. Dehlinger, S.P. Van, Shape of the hydrophobic barrier of phospholipid bilayers (evidence for water penetration in biological membranes), J. Membr. Biol. 15 (1974) 159–192, https://doi.org/10.1007/BF01870086.
[61] B. Valeur, Molecular Fluorescence: Principles and Applications, John Wiley & Sons, Ltd, 2001, https://doi.org/10.1002/3527600248.